

# Multi-Disaster Susceptibility Analysis on the Majene-Mamuju National Road Section Using a Geographic Information System Approach

Ahmad Reski Awaluddin<sup>1,\*</sup>, Nur Zahrah Afifah<sup>1</sup>, Ummu Kalsum Basman<sup>1</sup>, Firmansyah<sup>1</sup>, Wirmayanti<sup>1</sup>, Nurul Awwalul Fadliah<sup>1</sup>

<sup>1</sup> Faculty of Engineering, Universitas Sulawesi Barat, Majene, Indonesia

\* Corresponding Author E-mail: [ahmadreskiawaluddin@unsulbar.ac.id](mailto:ahmadreskiawaluddin@unsulbar.ac.id)

## Abstract

The Trans-Sulawesi National Road section Majene-Mamuju (segment 010–009) is a vital land transportation artery supporting the mobility and economy of over 475,000 people. However, its geographical profile, narrow coastal corridors adjacent to steep hills and active fault lines, exposes it to severe multi-hazard threats. This study establishes a fixed infrastructure inventory of 94.7 km of national road and 79 critical bridge nodes to assess susceptibility to earthquakes, tsunamis, coastal abrasion, and landslides. Spatial analysis derived from sub-district data tables reveals that earthquakes are the most pervasive threat, impacting 90.69 km (95.8%) of the road and 65 bridges (82.3% of the inventory). Tsunami susceptibility represents the second most significant hazard, threatening 56.71 km (59.9%) of the network and 51 bridges (64.6%). Coastal abrasion affects 25.20 km (26.6%) of the road and 47 bridges (59.5%). Landslides, while localized, present a high-intensity risk to 5.66 km (6.0%) of the road and 6 bridges (7.6%). The Sendana, Tammeroddo Sendana, and Tubo Sendana sub-districts emerge as the most critical multi-hazard zones, with composite indices ranging from 2.57 to 2.82. While Ulumanda exhibits a high landslide susceptibility ratio (13.0%), Sendana represents the primary operational threat with 1.83 km of exposed road, nearly double the absolute physical impact found in Ulumanda. These findings provide a standardized scientific basis for prioritizing structural mitigation at critical bridge nodes to prevent total network severance during cascading disaster events.

## Keywords:

Multi-hazard susceptibility, National Road; Majene-Mamuju; Disaster mitigation; Geographic Information System

## 1. INTRODUCTION

Indonesia, located on the Pacific Ring of Fire, consistently faces disaster challenges. Among its provinces, West Sulawesi stands out as the region with the highest disaster risk index (score 155.69) based on the 2024 National Disaster Risk Study (BNPB, 2025). The main threat in this coastal area comes from tectonic activity, particularly the Mamuju Thrust Fault, which has a maximum potential magnitude of up to M 6.6 (PUSGEN, 2017). This threat was evident on January 15, 2021, when an earthquake of M 6.2 struck Majene and Mamuju. This disaster not only claimed 73 lives but also triggered a cascading effect of landslides at over 60 locations, most of which completely blocked access to the Trans-Sulawesi arterial road, causing estimated economic losses of Rp 829.1 billion (Antara, 2021).

Road access plays a crucial role, not only in facilitating population mobility but also in ensuring the smooth distribution of logistics and the economy of a region (Rahayu, 2025). Therefore, roads become one of the main routes for distributing disaster relief (Boerboom et al., 2004). The Majene-Mamuju national road section (segment 010-009) serves as the only vital land transportation artery on the west coast of West Sulawesi. This route directly supports the mobility and economy of a total population of over 475,000 people

doi <https://doi.org/10.51557/yhjy774>

article history: Received October 12, 2025; Received in revised form February 09, 2026; Accepted February 24, 2026; Available online March 25, 2026.

This is an open access article under the [CC-BY-SA](https://creativecommons.org/licenses/by-sa/4.0/) license



in Majene and Mamuju districts (BPS Kabupaten Majene, 2024). Furthermore, this section is the main logistics corridor for economic activities, with a per capita GDP of Rp 53.93 million in Mamuju and Rp 35.33 million in Majene (BPS Kabupaten Majene, 2024). Access to the Majene-Mamuju national road section (segment 010-009) is frequently disrupted by landslides that block the entire road, especially during the rainy season from 2021 to 2023 (Hanafi, 2021; Hanapi, 2023; Himawan & Utomo, 2022), as well as by abrasion caused by high tides in 2020 (Hanapi, 2020). Considering the irreplaceable role of this road section, any disruption to it could paralyze logistics distribution, hinder access to emergency services, and limit evacuation routes during disasters. The road's characteristics, which largely follow the coastline and cut through hills, simultaneously expose it to threats from earthquakes, tsunamis, coastal abrasion, and landslides.

Existing disaster studies are often single-hazard, whereas in reality, disasters can occur in sequence or simultaneously (cascading effects). Therefore, research that integrates various types of threats (multi-hazard) is becoming increasingly important for a comprehensive understanding of risk. Although there have been studies examining multi-hazards, none have comprehensively combined geological and hydrometeorological threats in the way this research does. Some previous studies have tended to focus on different combinations of disasters or have significant data limitations. For example, (Mustikaningrum et al., 2023) analyzed floods, landslides, droughts, and earthquakes in the non-coastal areas of Gunungkidul. Similarly, Alwi et al. (2022) mapped the susceptibility to landslides, droughts, and floods in Semarang Regency. In a global context, Koks et al. (2019) analyzed the risks to road and railroad infrastructure from disasters such as tropical cyclones, earthquakes, and floods, but did not include landslides due to data limitations. Meanwhile, some other studies are more specific, such as Foralisa Toyfur et al. (2017) and Hosseini & Vayeghan (2008), which specifically focus on the danger of earthquakes to roads and bridges.

This research stands out by combining four major disasters relevant to the unique characteristics of the coastal region of West Sulawesi: earthquakes, tsunamis, coastal abrasion and landslides. By integrating these threats, this research offers a far more comprehensive and accurate understanding of disaster risks in this highly vulnerable region. This approach is a significant novelty compared to previous studies, which tended to be partial or focused on different types of hazards. This provides a stronger foundation for informed and effective mitigation planning. Therefore, this study aims to identify vulnerable zones along the Majene-Mamuju road section for each potential disaster (earthquake, tsunami, abrasion, and landslide), analyze the level of susceptibility spatially, and compile an integrated multi-hazard susceptibility map as an instrument for mitigation planning.

## **2. METHODS**

The research focused on the Trans-Sulawesi national road corridor, specifically the segment that connects Majene Regency with Mamuju Regency, West Sulawesi Province, road segment code 010-009 (Figure 1).

### **2.1 Study Area Characteristic**

This research was conducted on National Road 009-010, which connects Mamuju Regency and Majene Regency in West Sulawesi Province. Administratively, the route crosses eight (8) sub-districts, namely Banggae Timur, Banggae, Pamboang, Sendana, Tammeroddo Sendana, Tubo Sendana, Ulumanda, and Malunda, with a total road length of  $\pm 94.7$  km.

This road section is one of the main strategic routes because it serves as a link between the economic, social, and government activity centers in the northern and southern parts of West Sulawesi. Geographically, the research location is situated on the west coast of Sulawesi Island, bordering the Makassar Strait. Generally, the morphology of the study area is dominated by steep hills associated with active fault lines and a narrow coastal area vulnerable to tsunami and abrasion hazards. The combination of steep topography and high rainfall intensity also makes this area prone to landslides.

The selection of the research location was based on the high level of susceptibility to multi-hazards, including earthquakes, tsunamis, coastal abrasion, and landslides. Additionally, the presence of vital

infrastructure such as national roads and bridges along the Mamuju–Majene corridor makes this area a priority for disaster susceptibility studies.

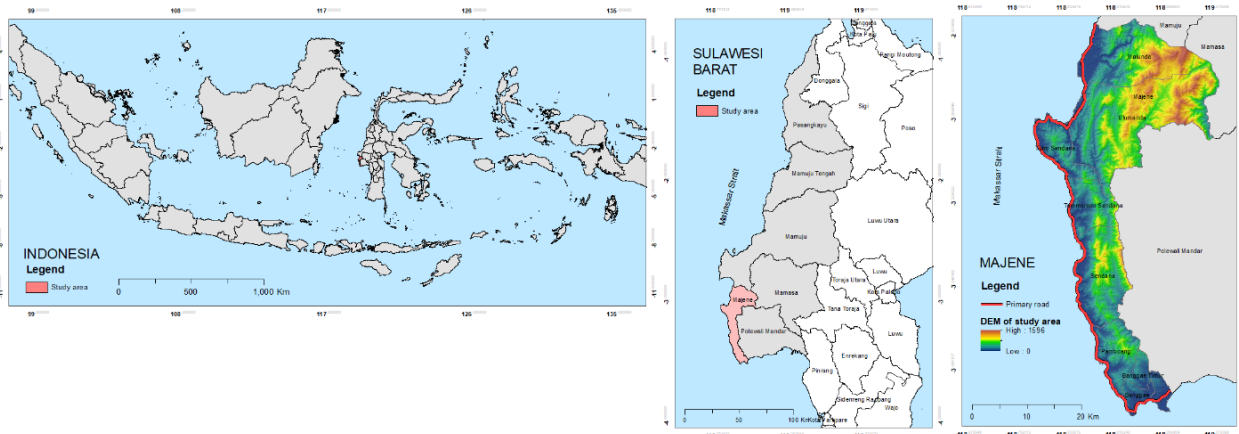


Figure 1. Research Location

## 2.2 Research Approach

This study uses a quantitative descriptive approach with spatial analysis based on Geographic Information System (GIS) software. The use of GIS software has been widely used for analyzes such as evaluating the suitability of residential land use (Rachmah et al., 2018), mapping the distribution of flood and landslide-prone areas (Irfan et al., 2023), analyzing the potential of agricultural land resources (Irfan et al., 2023), land management efficiency (Putri & Amrullah, 2024), and various other similar studies. This study analyzes four types of hazards: landslides, earthquakes, tsunamis and abrasion. The research framework for this study can be seen in Figure 2 below.

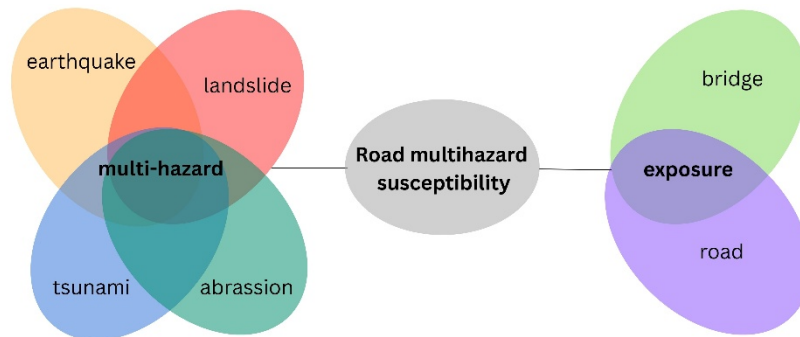


Figure 2. Research Approach

## 2.3 Datasets and Parameters

Each hazard has unique parameters derived from primary and secondary data. The type, source, and previous studies are described in Tables 1.

Table 1. Parameter Dataset

Parameter	Source	Empirical Studies
<b>HAZARD</b>		
<b>Landslide</b>		
Slope (DEM)	<a href="https://data.bris.ac.uk/">https://data.bris.ac.uk/</a>	(Elmoulat & Brahim, 2018; Khan et al., 2019; Kristiawan et al., n.d.; Sarkar et al., 2008; Sholichin et

Parameter	Source	Empirical Studies
		al., 2024; Vakhshoori & Zare, 2016)
Landslide susceptibility	<a href="https://geoportal.esdm.go.id/">https://geoportal.esdm.go.id/</a>	(Khan et al., 2019; Lee, 2019; Sarkar et al., 2008)
<b>Earthquake</b>		
Topography (DEM)	<a href="https://data.bris.ac.uk/">https://data.bris.ac.uk/</a>	(Ahmed et al., 2023; Jena et al., 2023; Yi et al., 2019; Zhou et al., 2019)
AVS30	National Center for Earthquake Study of Indonesia (PusGen)	(Amri et al., 2020; Triyatno et al., 2024)
Peak GA		
Shock intensity	National Center for Earthquake Study of Indonesia (PusGen)	(Amri et al., 2020; Triyatno et al., 2024)
Ground amplification factor		(Amri et al., 2020; Triyatno et al., 2024)
<b>Tsunami</b>		
Slope	<a href="https://data.bris.ac.uk/">https://data.bris.ac.uk/</a>	(Aslam et al., 2017, 2020; Safira et al., 2022; Sambah et al., 2018; Sambah & Miura, 2018)
Land cover	<a href="https://geoportal.menlhk.go.id/">https://geoportal.menlhk.go.id/</a>	(Römer et al., 2012; Steinritz et al., 2021)
Tsunami history	ESDM	(BNPB, 2021)
Coastline	<a href="https://tanahair.indonesia.go.id/">https://tanahair.indonesia.go.id/</a>	(Alwi & Mutaqin, 2022; Aslam et al., 2017, 2020; Sambah & Miura, 2018)
<b>Abrasion</b>		
Wave height	<a href="https://marine.copernicus.eu/">https://marine.copernicus.eu/</a>	(Naufal et al., 2019; Pratama et al., 2021)
Sea wave velocity	<a href="https://marine.copernicus.eu/">https://marine.copernicus.eu/</a>	(Naufal et al., 2019; Pratama et al., 2021)
Beach type	Google earth	(BNPB, 2021)
Beach line shape	Google earth	(BNPB, 2021)
Land cover	<a href="https://geoportal.menlhk.go.id/">https://geoportal.menlhk.go.id/</a>	(Naufal et al., 2019; Pratama et al., 2021)

Parameter	Source	Empirical Studies
<b>EXPOSURE</b>		
Length of Road	<a href="https://tanahair.indonesia.go.id/">https://tanahair.indonesia.go.id/</a>	(Hosseini & Vayeghan, 2008)
Number of bridge	Field survey	(Hosseini & Vayeghan, 2008)
Length of Bridge	Field survey	(Hosseini & Vayeghan, 2008)

## 2.4 Single Hazard Susceptibility of Road Mapping Methods

### 2.4.1 Landslide Susceptibility Index

The landslide hazard map was created using the Spatial Multi-Criteria Analysis (SMCA) approach. This method integrates two main datasets: the Digital Elevation Model (DEM) and the Landslide Susceptibility Zone Map. The analysis process begins by processing the DEM to obtain a slope class map, which is then combined with the susceptibility zone map to identify potential landslide zones. Areas with slope inclinations above 15% and 45% were mapped to identify areas with high landslide potential. These zones are then scored. In parallel, a runout analysis is performed to predict the sliding distance of landslide material, resulting in a runout potential zone that is also scored. These two scoring results are combined into one to produce a Landslide Hazard Index Map showing areas with different levels of landslide risk.

Table 2. Landslide Parameter Weighting

Parameter	Weight
Slope – Run out zone	0.6
Landslide susceptibility – Landslide zone	0.4

### 2.4.2 Earthquake Susceptibility Index

Earthquake hazard index maps are compiled by analyzing the effects of soil amplification. The process begins by processing DEM data to generate topographic classes. Separately, the AVS30 (shear wave velocity) values and the Peak Ground Acceleration (PGA) Map at bedrock were prepared. The AVS30 values were adjusted for topographic class to calculate the soil amplification factor, which indicates how much the shaking will be amplified. Simultaneously, the PGA values were processed to obtain continuous values across the entire study area. The result is that the soil amplification factor is multiplied by the PGA value to produce an estimate of peak acceleration at the surface. This estimate is a representation of the Earthquake Hazard Index Map.

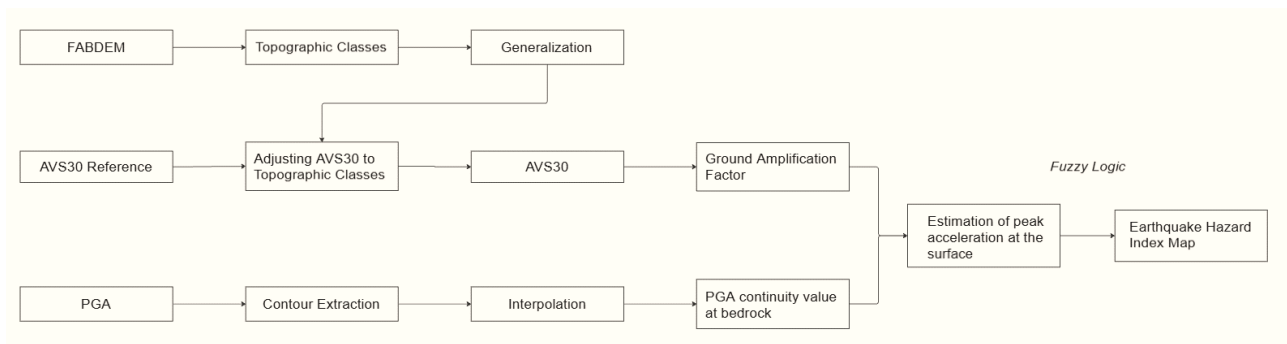


Figure 3. Earthquake Hazard Indexing Method

### 2.4.3 Tsunami Susceptibility Index

To create a tsunami hazard map, spatial analysis was used to model flood areas by considering several parameters. This analysis begins by processing DEM data, land cover, maximum tsunami height, and coastline. From the DEM, the slope was calculated. Land cover data was used to calculate the surface roughness coefficient. These two results are used to calculate the wave energy loss rate (Hloss). The value of Hloss is then used to model the inundation distance, which produces an inundation map. This map was then analyzed using fuzzy logic to account for uncertainty, ultimately resulting in a Tsunami Hazard Index Map. This map is very important for coastal mitigation and evacuation planning.

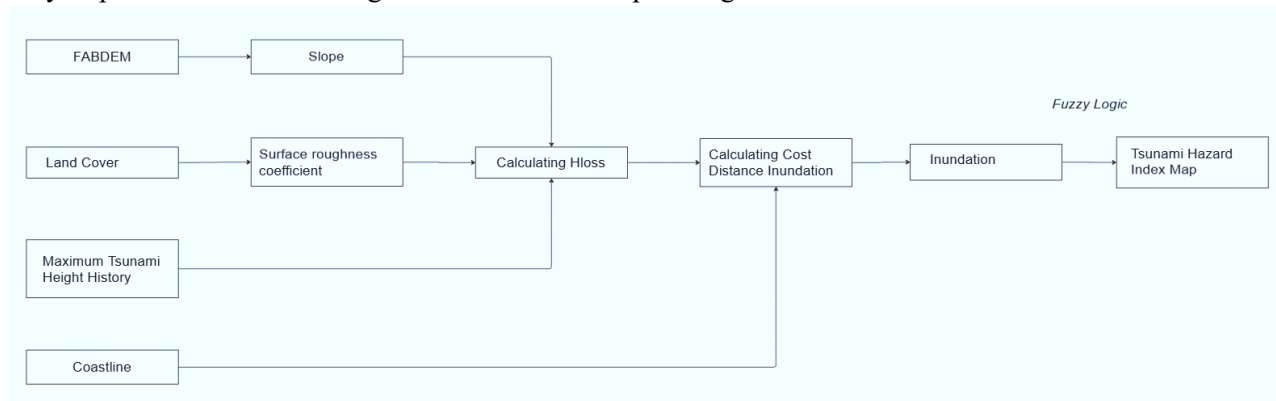


Figure 4. Tsunami Hazard Indexing Method

### 2.4.4 Abrasion Susceptibility Index

The abrasion hazard index map was created by analyzing five main factors influencing erosion: wave height data, sea current velocity, geomorphological maps, land cover maps, and the coastline. Each of these data points is classified, scored, and weighted according to its level of importance. After all criteria are assessed, the entire data layers are combined using a process. This analysis is limited to an area within 25 meters of the coastline to focus on the most vulnerable zone. The result of this process is the Coastal Erosion Hazard Index Map, which serves as an important guide for policymakers in managing and protecting coastal areas from the threat of erosion.

Table 3. Abrasion Parameter Weighting

Parameter	Weight
Wave height	0.3
Sea wave velocity	0.3
Beach type	0.1
Beach line shape	0.15
Land cover	0.15

### 2.4.5 Single Hazard Susceptibility of Road

The susceptibility analysis of national road to natural disasters was conducted by integrating road and bridge network data into the hazard maps that had been prepared. This process begins by overlaying road data with high-hazard zone maps for each type of disaster (landslides, tsunamis, earthquakes and coastal erosion). Through spatial analysis, the length of roads and the number of bridges exposed in these high-risk zones were identified and measured. This measurement was then used to calculate the ratio of exposed road length and

number of bridges to the total network. The four resulting parameters, road length, exposed road length ratio, number of bridges, and exposed bridge number were then scored and weighted according to their importance. These scores and weights are combined to obtain the final risk value for each road segment. The result is a susceptibility level classification showing zones from "low" to "high" for each type of disaster.

Table 4. Single Hazard Susceptibility of Road Parameter Weighting

Parameter	Weight
Length of Bridges Exposed to High Susceptibility (m)	0.2
Length of Roads Exposed to High Susceptibility (km)	0.1
Ratio of Exposed Roads to Road Length (%)	0.4
Number of Bridges Exposed to High Susceptibility	0.3

## 2.5 Multi-Hazard Susceptibility of Road Mapping

After analyzing the susceptibility to each disaster individually, the next step is to combine all these results into a comprehensive multi-hazard map. This process is done by combining the susceptibility scores from each disaster, landslides, tsunamis, earthquakes, and coastal erosion for each road segment. This combination is done through a weighting process, where each type of disaster is given a relative weight according to its level of urgency or potential impact. By summing these weighted susceptibility scores, a total susceptibility index is produced.

Table 5. Multi-Hazard Susceptibility of Road Parameter Weighting

Hazard	Weight
Landslide	0.1064
Earthquake	0.1064
Tsunami	0.1064
Abrasion	0.1064

Modified PerkaBNPB No. 2 Tahun 2012

$$\text{Multihazard Susceptibility} = \left( H_{\text{Landslides}} \times \frac{0.1064}{0.4256} \right) + \left( H_{\text{Earthquake}} \times \frac{0.1064}{0.4256} \right) + \left( H_{\text{Tsunami}} \times \frac{0.1064}{0.4256} \right) + \left( H_{\text{Abrasion}} \times \frac{0.1064}{0.4256} \right)$$

## 2.6 Methodological Justification for Parameter and Hazard Weighting

The determination of weights in this study follows a structured approach that integrates national regulatory standards with researcher assumptions tailored to the specific geographical context of West Sulawesi. Individual Parameter Weighting (Tables 2, 3, and 4): The weights assigned to individual parameters for landslide, abrasion, and road susceptibility were adopted from the PerkaBNPB No. 2 Tahun 2012. For landslides, the Slope – Run out zone is weighted most heavily at 0.6 because steep topography (exceeding 45% in critical segments) is scientifically identified as the primary trigger for mass movement along the Majene-

Mamuju corridor. Similarly, for coastal abrasion, wave height and sea wave velocity are given the highest weights (0.3 each) as they represent the fundamental energy drivers of coastal erosion.

In evaluating road susceptibility (Table 4), the Ratio of Exposed Roads (0.4) and the Number of Bridges (0.3) are prioritized over absolute road length. This is based on the infrastructural logic that bridges represent critical nodes; while road surfaces may be cleared of landslide debris, the failure of a bridge represents a total severance of the only vital land transportation artery for over 475,000 people.

Multi-Hazard Index Weighting (Table 5): The Multi-hazard Susceptibility Index was calculated using a Modified PerkaBNPB No. 2 Tahun 2012 approach, where each of the four primary hazards (landslides, earthquakes, tsunamis, and abrasion) was assigned an equal weight of 0.1064. This equal distribution is based on a specific researcher assumption: given that West Sulawesi possesses the highest disaster risk index in Indonesia (score 155.69), all four hazards carry a near-equal level of urgency for infrastructure resilience. In this high-risk environment, a single-hazard focus is insufficient because geological and hydrometeorological threats often overlap. By applying equal weights, the study ensures that the multi-hazard map holistically identifies "High Susceptibility" zones where these threats converge, most notably in the Sendana, Tammeroddo Sendana, and Tubo Sendana sub-districts.

This weighting strategy moves the analysis beyond a simple inventory by providing a standardised and reproducible framework aligned with Indonesian national disaster management protocols, while remaining sensitive to the unique multi-hazard profile of the Trans-Sulawesi National Road

### **3. RESULT AND DISCUSSION**

#### **3.1 Spatial mapping of parameters**

The research focused on the Trans-Sulawesi National Road corridor, specifically the segment that connects Majene Regency with Mamuju Regency, West Sulawesi Province, with road segment code 010-009. Spatial analysis shows different susceptibility distributions for each type of disaster.

##### **3.1.1 Landslide Susceptibility Parameters Mapping**

This landslide zone reflects a combination of various factors such as soil type, land cover, and rainfall, all of which contribute to the potential for landslides. The landslide zone map and data serve as a synthesis of all analyzes. After considering all factors, the total area at high landslide risk increased to 179.02 km<sup>2</sup>. This figure is significantly larger than the area with high slope gradients (92.57 km<sup>2</sup>), indicating that other factors, such as soil conditions, vegetation cover, and hydrology, play a crucial role in increasing landslide risk in areas that may not have extreme slope gradients (Khan et al., 2019; Sholichin et al., 2024). Thus, this comprehensive analysis not only identifies where the highest landslide risks are located but also highlights how the combination of various factors can significantly expand the hazard zone.

##### **3.1.2 Tsunami Susceptibility Parameters Mapping**

The threat of a tsunami is determined not only by the wave itself, but also by how the wave interacts with the land. The analysis results indicate that various geographical factors play a key role in determining the level of threat. The slope gradient map (Sin Slope) highlights areas with gentle slopes tend to be more susceptible to widespread flooding. These factors, both those that slow down and those that speed up the wave, must be deeply understood for effective mitigation planning.

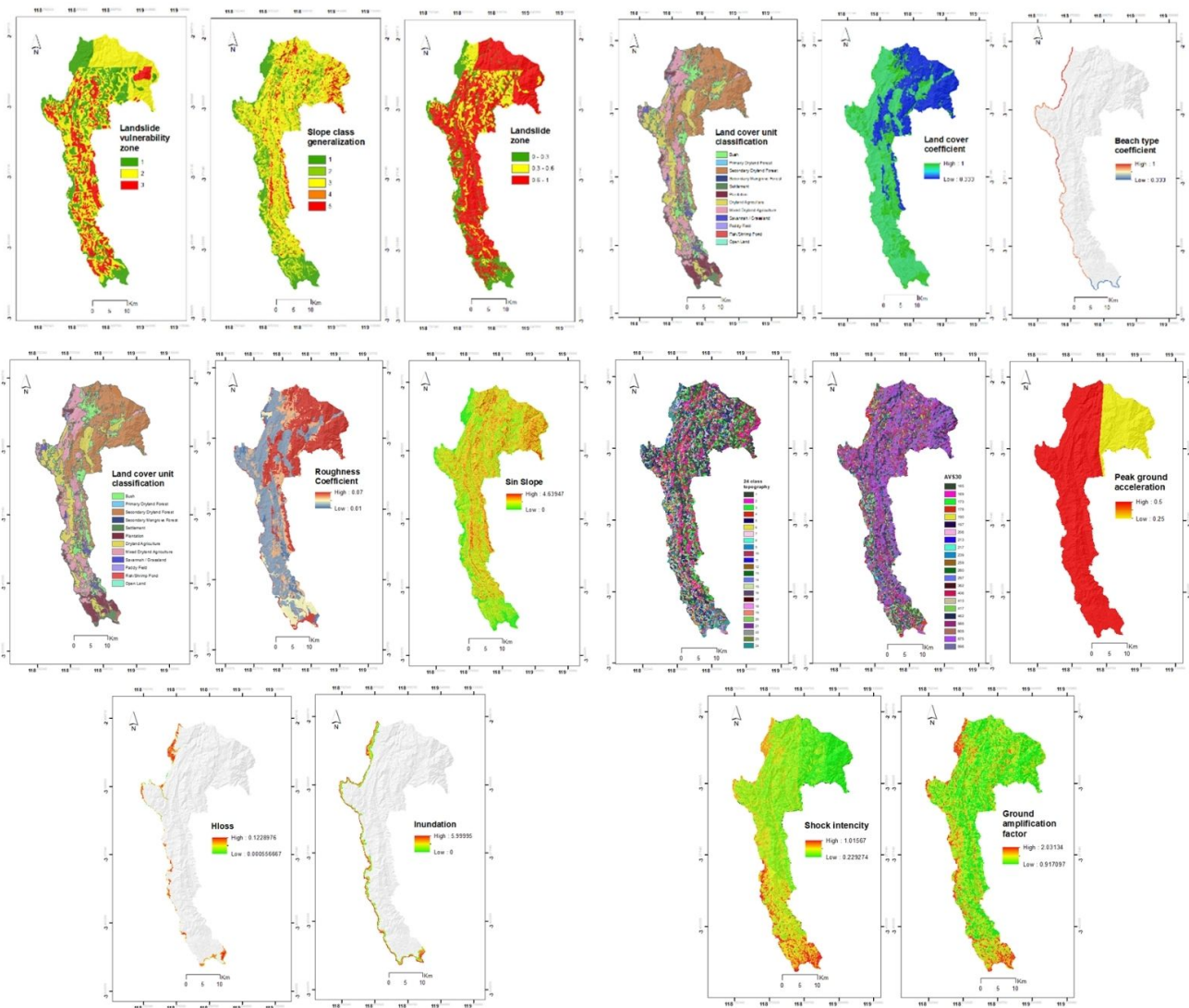


Figure 5. Parameter Maps

The disparity between the area size and extreme wave height and the area size and high flooding is a key finding of this analysis. This means that although the waves did not reach extremely high heights in most areas, the gentle topography and other geographical features caused the water to spread far inland. In other words, the main threat to this region is not destructive wave height, but the extent of the flooded area. The majority of historical destruction occurred in flat areas that provided little barrier to the free-flowing tsunami waves (Biswas & Sil, 2023)

### 3.1.3 Earthquake Susceptibility Parameters Mapping

The Peak Ground Acceleration (PGA) map shows the maximum ground acceleration during an earthquake, which is a key indicator of shaking intensity. Based on the map, most of the area, especially the southern part, is indicating a high PGA level. Conversely, areas of low acceleration cover less, indicates that the region has the potential for very strong and widespread earthquake shaking.

The Shock Intensity map and data describe how strongly the earthquake was felt on the surface. Although most areas have high acceleration, the ground motion intensity data shows a different pattern. The area with moderate intensity is the largest. This disparity indicates that other factors, such as soil characteristics, can influence how the shaking is felt, even the earthquake that occurred was of great magnitude.

The Ground Amplification Factor explain how local soil conditions can amplify seismic waves (Jena et al., 2023). Soft soil or sediment, for example, can significantly amplify earthquake shaking, even if the

earthquake originates from a distance. Quantitative data shows that areas with a medium amplification factor are the most extensive, while areas with a high amplification factor have less, which is quite significant. This finding is crucial because it shows that even though the earthquake wasn't very strong, areas with high amplification factors are still at risk of experiencing damaging shaking.

### 3.1.4 Abrasion Susceptibility Parameters Mapping

The map shows the classification of different land cover units, ranging from forests and agricultural land to settlements. This land cover plays a crucial role in mitigating abrasion. Natural vegetation such as mangrove forests and coral reefs can act as natural protectors, absorbing the energy of ocean waves. The land cover coefficient, quantifies this protective role. High coefficient values indicate effective land cover in preventing abrasion, such as densely forested areas (Ustaoğlu et al., 2021). Conversely, areas with low show less effective land cover, such as open land or agricultural areas, which are more susceptible to abrasion.

The beach type coefficient, focuses on the physical characteristics of the coastline itself. This parameter assesses how vulnerable the beach is to wave erosion. High coefficient values indicate beach types that are highly susceptible to abrasion, such as sandy beaches (Naufal et al., 2019) or beaches that have already been damaged. Low coefficient values indicate more stable and abrasion-resistant beach types, such as rocky or coral beaches. This map shows that most of the coastline in this region has a high coefficient, indicating widespread and serious abrasion risk.

## 3.2 Single Hazard Susceptibility Index

The hazard index map shows the spatial distribution of landslide, earthquake, tsunami, and abrasion susceptibility on Majene Regency. Generally, the susceptibility pattern indicates an overlap of multi-disaster threats across most of the study area.

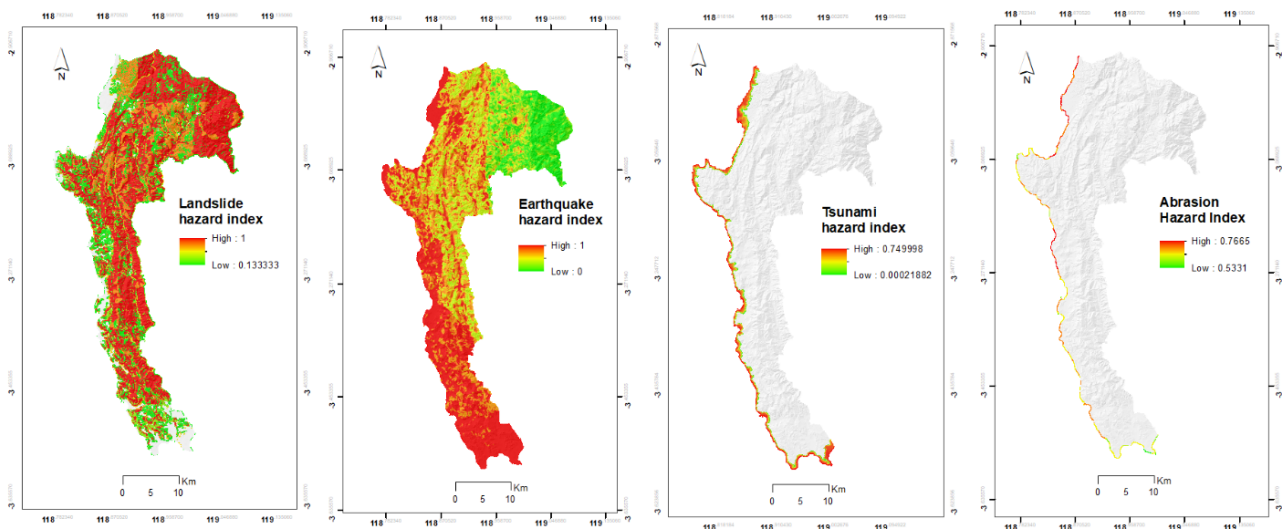


Figure 6. Single Hazard Susceptibility Index

Regarding landslide hazards, the hazard index map shows a dominance of the high class in hilly areas, particularly in the central to southern parts of the study area. This is consistent with the steep topography and lithology that is susceptible to weathering. Landslides frequently occur on steep slopes where powerful tectonic movements and weathering have produced an abundance of loose regolith and soil (He & Beighley, 2008). The road segments cutting through steep slopes in Pamboang, Sendana, and Ulumanda sub-districts are located in a high-risk zone, making them highly susceptible to disruption during heavy rainfall.

For earthquakes, the spatial distribution shows that almost the entire central to southern part of the study area falls into the high-risk category. High class dominates, especially along the coastal and hilly areas associated with active fault lines. The high peak ground acceleration values were dominant. Thus, the national road segment from Majene to Malunda is highly susceptible to the impact of earthquake shocks. The highest

earthquake hazards are found in areas where high PGA values were dominant and statistical analysis confirmed that these values substantially affected the magnitude of the earthquake hazard (Triyatno et al., 2024).

The danger of tsunamis is indicated by a high susceptibility index along the coastline, particularly in the southwestern part of the study area. The dominant high class in the coastal segment confirms the high potential for flooding in areas with gentle morphology and minimal vegetation cover. It has been proven that for a lower roughness coefficient (indicating minimal vegetation or smooth surfaces), a tsunami can travel further inland than in areas with higher coefficients (Steinritz et al., 2021). This is consistent with the historical records of the 1967 and 1969 tsunamis that previously struck this area.

With the national road being located close to the coast, the abrasion hazard index map shows high susceptibility concentrated along the coastline in Pamboang, Sendana, and Malunda districts. The section of national road parallel to the coastline zone with a high susceptibility index, indicating potential active erosion due to sea waves and longshore currents. Although the affected area is relatively small compared to other disasters, the threat of abrasion is chronic and directly impacts the sustainability of coastal road infrastructure. Disasters related to coastal dynamics can devastate both onshore and offshore infrastructure, resulting in significant economic losses (Al Hakim et al., 2025).

Table 6. Single Hazard Susceptibility Class and Area

Class	Landslide hazard index (area in Km <sup>2</sup> )	Earthquake hazard index (area in Km <sup>2</sup> )	Tsunami hazard index (area in Km <sup>2</sup> )	Abrasion hazard index (area in Km <sup>2</sup> )
<b>Low</b>	144,47	157,83	5	-
<b>Medium</b>	53,37	238,93	21	0,45
<b>High</b>	573,77	497,65	20	5,33

### 3.2.1 Road susceptibility to landslide hazard

The analysis results shows several segments with a high level of susceptibility to landslides (Table 7). Landslide susceptibility is highly concentrated in hilly regions with steep slopes exceeding 15% and 45%. Although the total length of road segments exposed to high landslide risk is relatively small, 5.66 km or 6.0% of the total network, the risk is critical because landslides can instantaneously sever transportation access.

The analysis shows that the study area is at high landslide risk, influenced by a combination of steep topography, weathered lithology, and limited vegetation. Spatially, Ulumanda District exhibits the highest susceptibility ratio (13.07%), while Sendana District contains the longest segment of landslide-prone road at 1.83 km. Bridge infrastructure is also impacted, with six units located in high-risk zones, five of which are in Tubo Sendana.

Table 7. Road Susceptibility Parameters to Landslide Hazard

Route (subdistrict)	Length of Roads Exposed to High Landslide Susceptibility (km)	Ratio of Exposed Roads to Road Length (%)	Number of Bridges Exposed to High Landslide Susceptibility
<b>Banggae Timur</b>	0	0	0
<b>Banggae</b>	0	0	0
<b>Pamboang</b>	0.79	4.8	0
<b>Sendana</b>	1.83	9.3	0

<b>Tammeroddo Sendana</b>	0.71	6.2	0
<b>Tubo Sendana</b>	1.05	4.8	5
<b>Ulumanda</b>	0.95	13.0	0
<b>Malunda</b>	0.33	2.3	1

### 3.2.2 Road Susceptibility to Earthquake Hazards

The research identifies earthquakes as the most pervasive threat to the national road corridor, exhibiting the widest geographical scope and the highest susceptibility levels. Spatial modeling of Peak Ground Acceleration (PGA) indicates that high acceleration zones dominate approximately 689.94 km<sup>2</sup> of the study area, particularly in the southern regions associated with active fault lines.

The impact on infrastructure is severe: 90.69 km (approximately 95.8%) of the total road length is categorized as highly vulnerable. Furthermore, 65 bridges are situated within these high-risk zones, with the highest concentrations found in the Sendana (18 bridges), Tubo Sendana (12 bridges), and Malunda (11 bridges) sub-districts. This widespread susceptibility is exacerbated by local soil amplification factors, where soft sediment can significantly intensify seismic waves even if the earthquake originates from a distance.

With almost universal susceptibility, earthquakes can be categorized as a dominant threat to National Road 009–010. The implication of this condition is the need to implement earthquake-resistant infrastructure technical standards, for both roads and bridges.

Table 8. Road Susceptibility Parameters to Earthquake Hazard

Route (subdistrict)	Length of Roads Exposed to High Earthquake Susceptibility (km)	Ratio of Exposed Roads to Road Length (%)	Number of Bridges Exposed to High Earthquake Susceptibility
<b>Banggae Timur</b>	4.44	99.4	2
<b>Banggae</b>	8.26	98.9	2
<b>Pamboang</b>	15.69	96.2	6
<b>Sendana</b>	18.44	93.9	18
<b>Tammeroddo Sendana</b>	9.97	87.8	11
<b>Tubo Sendana</b>	16.69	77.1	12
<b>Ulumanda</b>	4.21	57.9	3
<b>Malunda</b>	12.99	92.5	11

### 3.2.3 Road Susceptibility to Tsunami Hazards

The threat of tsunamis is primarily concentrated along the western coastline, where gentle morphology and minimal vegetation cover facilitate extensive inland flooding. A critical finding of the study is the disparity between wave energy and flooding extent; while the area experiencing extreme wave height (High Hloss) is limited to 0.45 km<sup>2</sup>, the high inundation zone reaches 20 km<sup>2</sup>. This suggests that the primary threat is not necessarily wave height, but the propensity for water to spread far inland due to topographical features.

Infrastructure exposure to tsunamis is significant, with 56.71 km (59.9%) of the national road classified as highly susceptible. The sub-districts of Sendana and Tubo Sendana are the most vulnerable, collectively containing 30 bridges located within high tsunami risk zones

Table 9. Road Susceptibility Parameters to Tsunami Hazard

Route (subdistrict)	Length of Roads Exposed to High Tsunami Susceptibility (km)	Ratio of Exposed Roads to Road Length (%)	Number of Bridges Exposed to High Tsunami Susceptibility
<b>Banggae Timur</b>	0.73	16,4	2
<b>Banggae</b>	3.14	37,5	1
<b>Pamboang</b>	10.02	61,4	2
<b>Sendana</b>	15.52	79,1	16
<b>Tammeroddo Sendana</b>	6.32	55,6	11
<b>Tubo Sendana</b>	13.48	62,3	14
<b>Ulumanda</b>	0.45	6,2	0
<b>Malunda</b>	7.05	50,2	5

#### 3.2.4 Road Susceptibility to Abrasion Hazards

Coastal abrasion represents a chronic threat to the sustainability of road infrastructure, particularly in areas where the road is parallel to the coastline. The susceptibility is largely determined by beach type and land cover; sandy or damaged beaches show high coefficients of vulnerability, whereas natural protectors like mangrove forests are more resilient.

The study identifies 25.2 km of road as being highly susceptible to abrasion. The threat is most concentrated in Tubo Sendana (7.05 km), Sendana (6.79 km), and Tammeroddo Sendana (4.46 km). Collectively, 36 bridges are threatened by coastal erosion in these areas, highlighting the need for specialized mitigation strategies focused on protecting vital transportation nodes from wave-induced damage.

Table 10. Road Susceptibility Parameters to Abrasion Hazard

Route (subdistrict)	Length of Roads Exposed to High Abrasion Susceptibility (km)	Ratio of Exposed Roads to Road Length (%)	Number of Bridges Exposed to High Abrasion Susceptibility
<b>Banggae Timur</b>	0,31	6,9	0
<b>Banggae</b>	0	0	1
<b>Pamboang</b>	3,41	20,9	4
<b>Sendana</b>	6,79	34,6	12
<b>Tammeroddo Sendana</b>	4,46	39,3	10
<b>Tubo Sendana</b>	7,05	32,6	14
<b>Ulumanda</b>	0,38	5,3	1
<b>Malunda</b>	2,80	19,9	5

### 3.3 Single Hazard Susceptibility Index on the Majene – Mamuju National Road Section

Based on the analysis results (Figure 7), the threat of landslides on arterial roads is not evenly distributed across the entire area, but is concentrated in hilly regions. Data shows that although the total length of landslide-prone roads is relatively small (5.66 km), some sub-districts have high susceptibility. The map clearly visualizes these findings with red areas (high susceptibility) scattered along road sections in Sendana and Tubo Sendana, which have significant lengths of vulnerable roads. While landslide risk is distributed unevenly, Sendana sub-district represents the primary operational threat to the national road network, containing 1.83 km of high-susceptibility road, the longest continuous hazard segment in the study area. Although Ulumanda exhibits the highest localized risk density (13.0%), the absolute physical impact in Sendana is nearly double, representing a significantly larger burden for emergency clearance and structural mitigation.

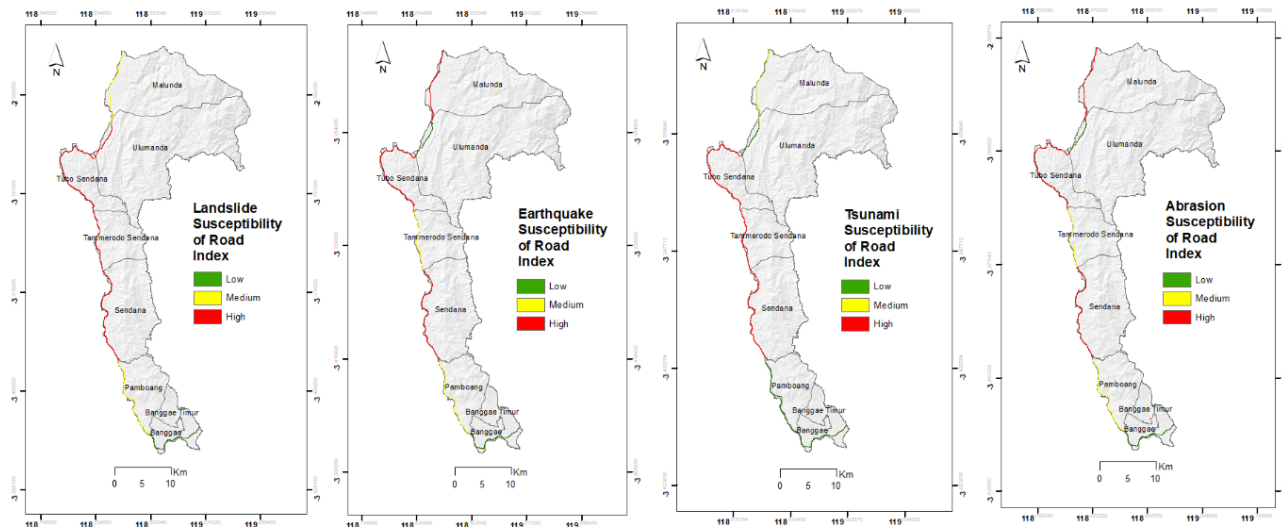


Figure 7. Single Hazard Susceptibility Index on the Majene – Mamuju National Road Section

Earthquakes represent the most pervasive hazard within the study area, with high-susceptibility zones encompassing 90.69 km (95.8%) of the national road length,. While the threat to the road surface is near-universal, the impact on structural nodes is more concentrated: 65 out of the total 79 bridges (82.3%) are located in high-risk earthquake zones. This distinction is critical for infrastructure planning, as it reveals that 14 bridges (17.7% of the inventory) are situated in segments with lower susceptibility levels,. These safer nodes are primarily found in sub-districts like Banggae Timur, Banggae, and Ulumanda, which maintain lower multi-hazard indices,. Consequently, while the vast majority of the network faces severe seismic risk, the 17.7% of bridges outside high-hazard zones represent pockets of relative structural resilience within the corridor

Tsunami susceptibility specifically focuses on coastal areas. The data table shows that the total length of national roads vulnerable to tsunamis is 56.71 km. The Tsunami Susceptibility Map reinforces this finding by visualizing thick red areas along roads adjacent to the coastline. Sendana sub-district is the most threatened, with 15.52 km of high-risk roads and 16 bridges located in the risk zone. The visualization on this map shows that the tsunami threat is very serious for the sustainability of coastal road functions, and has the potential to cut off transportation access and damage vital bridge infrastructure, as seen in the data.

Just like tsunamis, abrasion is a very significant threat to coastal road infrastructure. The data table records a total of 25.2 km of road highly susceptible to abrasion, with the largest concentrations in Tubo Sendana, Sendana, and Tammeroddo Sendana. The Abrasion Susceptibility Map visually supports this data, displaying road paths in the subdistrict in a deep red color. This visualization emphasizes that coastal erosion is a major cause of road damage, especially in areas directly exposed to sea waves. This finding is important for mitigation planning focused on protecting the roads and bridges (47 in total) threatened in these areas.

### 3.4 Multi-hazard Susceptibility Index on the Majene – Mamuju National Road Section

The analysis results show significant variations in risk levels along this road section, with most areas falling into the high and medium susceptibility categories, while a small portion is low susceptibility (Table 11). This finding confirms that this national road section as a whole faces complex vulnerabilities to various natural disaster threats simultaneously.

Table 11. Multi-hazard Susceptibility of Road Index

Section	Route	Susceptibility Index of Road					Multi-hazard	Multi-hazard Susceptibility of Road Index
		Landslide	Earthquake	Tsunami	Abrasion	Multi-hazard		
010	Banggae Timur	1	1,8	1	1,5	1,325	Low	
	Banggae	1,1	1,6	1,5	1,1	1,325	Low	
	Pamboang	1,4	2,5	1,8	2,5	2,05	Medium	
	Sendana	2	3,3	3	3	2,825	High	
	Tammeroddo Sendana	2	3	2,6	2,7	2,575	High	
009	Tubo Sendana	2,2	3	2,6	3	2,7	High	
	Ulumanda	1,9	1,5	1,1	1,5	1,5	Low	
	Malunda	1,6	3	1,9	2,7	2,3	Medium	

The analysis results clearly map the areas at highest risk (Figure 8). There are three sub-districts categorized as having a high level of susceptibility, namely Sendana, Tammeroddo Sendana, and Tubo Sendana. This highest susceptibility is indicated by the multi-disaster index value, which falls in the range of 2.575 to 2.825. This figure is driven by a very high combination of landslide and earthquake index values, along with significant potential threats of tsunamis and abrasion. This indicates that the road segments in these three regions are the most critical and require serious attention in mitigation efforts and infrastructure planning.

Meanwhile, the other two sub-districts, Pamboang and Malunda, are considered to have moderate susceptibility. The multi-hazard index in this region ranges from 2 to 2.3. Although not as prone to disasters as other regions, this risk level still requires vigilance, especially considering the potential threats of earthquakes and abrasion, which are quite prominent. On the other hand, the analysis found that three sub-districts had low susceptibility, namely Banggae Timur, Banggae, and Ulumanda. This region has a multi-hazard index below 2.0, indicating that the road sections here are relatively safer from the combined existing disaster threats compared to other areas along the corridor.

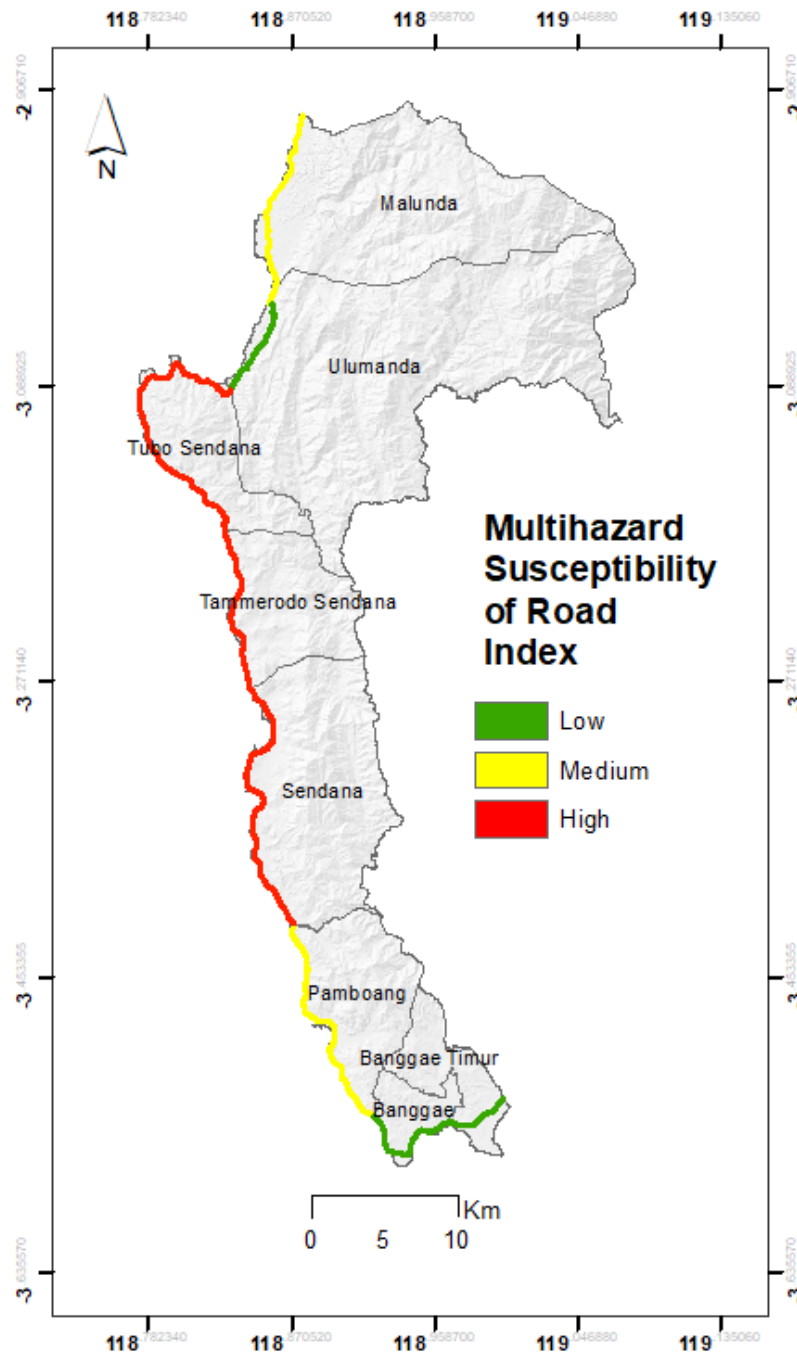


Figure 8. Multi-hazard Susceptibility of Road Index

A sensitivity analysis was performed to evaluate the dominance of the earthquake hazard. Results show that even when earthquake weights are reduced by 50%, the Sendana-Tubo Sendana corridor remains in the high-susceptibility category. This confirms that the multi-hazard risk in this segment is a result of compound vulnerabilities, where steep slopes and coastal exposure coincide with seismic faults, rather than a bias from the dominant earthquake dataset

Overall, these findings provide a strong foundation for strategic decision-making. With these detailed maps and data, the government and relevant parties can prioritize resource allocation for disaster mitigation, such as building landslide retaining structures or early warning systems, focusing on areas with the highest levels of susceptibility. This multi-hazard approach is crucial because it helps identify risks holistically, allowing prevention efforts to be more effective and targeted.

### 3.5 Validation

The results of the road susceptibility analysis for landslides and abrasion were validated through field documentation presented on maps (Figure 9). On the landslide hazard map, the distribution of hazard classifications along the Majene–Mamuju National Road section is visible. The red-colored segment indicates high susceptibility, which is dominant in steep slope areas, particularly in the sub-districts of Pamboang, Sendana, Tammeroddo Sendana, and Tubo Sendana. Field documentation (L001–L014) shows the actual conditions, including steep cliffs, landslide material on the road shoulder, and cracks in the road surface, which are consistent with the results of spatial modeling. This reinforces the fact that steep topography, weathered lithology, and limited vegetation are the main triggers for landslide susceptibility along this section.

Meanwhile, the abrasion susceptibility map shows a concentration of red-colored segments on roads directly associated with the coastline. The field validation points (A001–A021) show the real conditions, including damage to the road body caused by sea waves, loss of shoulder material, and coastal line shifts. High-risk locations are found in abundance in the sub-districts of Pamboang, Sendana, and Tubo Sendana, where the coastline is relatively narrow and directly faces high waves.

Overall, this validation demonstrates consistency between the results of GIS-based spatial analysis and field conditions. The resulting susceptibility map can be said to be representative in depicting the potential for disruption to road infrastructure due to landslides and abrasion, making it suitable as a basis for mitigation planning and construction reinforcement in critical segments.

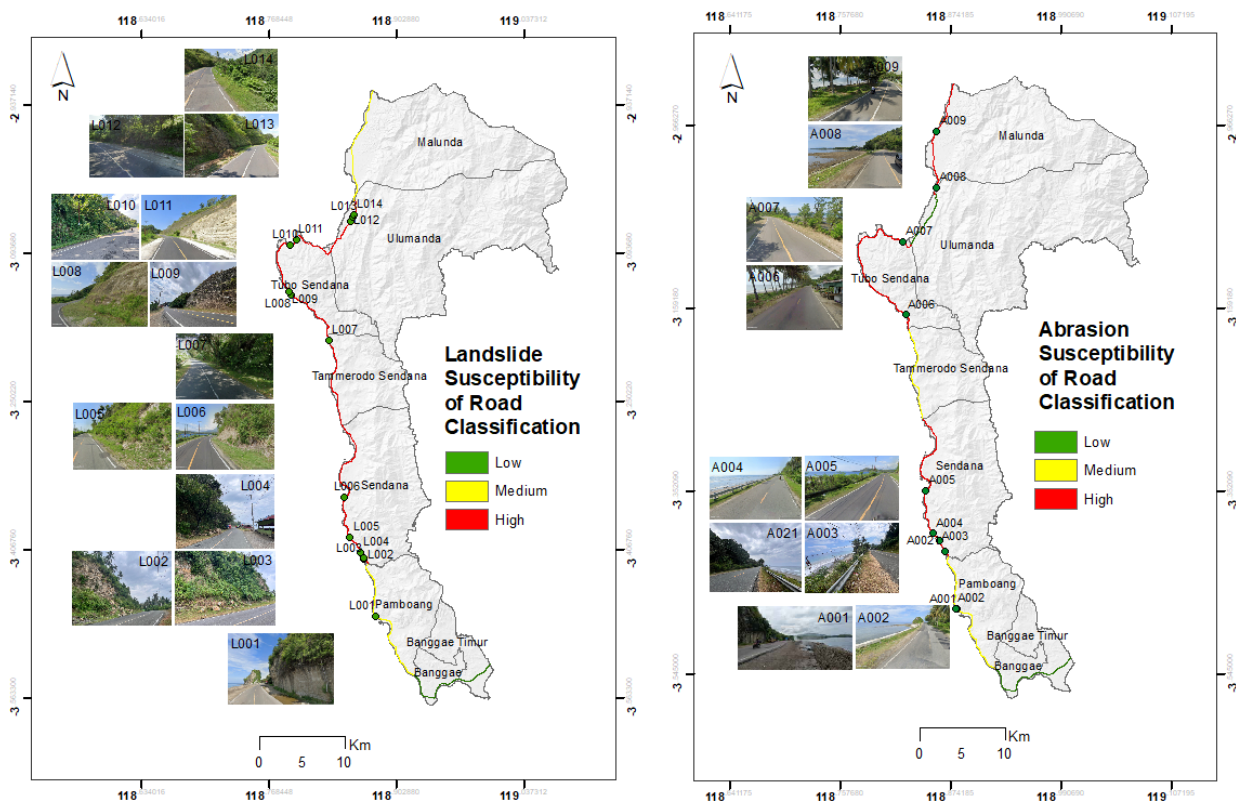


Figure 9. Field validation map

### 3.6 Analysis of Cascading Effects and Compound Risk

While this study utilizes a weighted linear summation to determine the Multi-hazard Susceptibility Index, it is crucial to acknowledge that in the unique geographical context of West Sulawesi, disasters rarely occur in isolation. Cascading effects, where a primary hazard triggers a chain of secondary disaster (Tansel, 2025), represent a significant threat to the Majene-Mamuju national road corridor.

The reality of these complex interactions was demonstrated during the January 2021 M 6.2 earthquake, which served as a primary trigger for a series of secondary events (Meilano et al., 2023). This seismic activity

did not merely cause ground shaking; it triggered landslides at over 60 locations, which effectively paralyzed the Trans-Sulawesi arterial road and hindered emergency logistics. This specific sequence illustrates how earthquake susceptibility (which dominates 95.7% of the road length) directly amplifies landslide risk in real-time, regardless of rainfall conditions. Furthermore, in segments where the road is narrow and adjacent to the coastline, such as in Sendana and Tubo Sendana, the degradation of these protections immediately increases susceptibility to coastal abrasion and reduces the land's natural resilience against tsunami inundation (Naufal et al., 2019).

By treating these hazards as a linear sum in the current methodology, there is a risk of underestimating the compound impact where hazards reinforce one another. For instance, a road segment categorized as "Medium" susceptibility might experience "High" impact if a landslide blocks an evacuation route during a tsunami. Therefore, the high susceptibility scores identified in the Sendana, Tammeroddo Sendana, and Tubo Sendana sub-districts (indices 2.57 to 2.82) should be interpreted not just as an inventory of separate threats, but as a zone of potential compound disaster chains. However, while equal weighting of hazards is noted to lead to conservative classifications and potential underestimation, some dynamic weighting strategies could potentially lead to an overestimation of exposure if they do not account for the fact that secondary hazards are often conditional on a primary trigger (Castiglione et al., 2026).

This scientific perspective shifts the understanding of road vulnerability from a static inventory to a dynamic system. Future mitigation for the Majene-Mamuju section must move beyond single-hazard structural reinforcements and consider multi-hazard interactions, ensuring that earthquake-resistant designs also account for the increased lateral pressure of seismically-triggered landslides.

#### **4. CONCLUSION**

This research shows that the Majene–Mamuju National Road section (segment 010–009) is vulnerable to various types of disasters, with earthquakes, tsunamis, abrasion, and landslides being the dominant threats. GIS-based spatial analysis successfully identified critical zones that need to be prioritized for mitigation, especially in the Sendana, Tammeroddo Sendana, and Tubo Sendana areas, which have a high multi-disaster susceptibility index. Meanwhile, the Banggae Timur, Banggae, and Ulumanda areas are relatively safer with a low level of susceptibility.

This result underscores the importance of integrated mitigation measures through disaster-resilient infrastructure development, strengthening early warning systems, and adaptive spatial planning. The limitations of this study are that it still relies on the availability of secondary data, which may have limited resolution. Therefore, further research is recommended to involve detailed field surveys and the integration of the latest data to improve the accuracy of the susceptibility map.

#### **5. LIMITATION & FUTURE RESEARCH**

The primary limitation is the use of a weighted linear summation to form the multi-hazard index. This methodology assumes that hazards, landslides, earthquakes, tsunamis, and abrasion, act independently. In reality, these disasters often trigger one another, such as the January 2021 earthquake which caused over 60 landslides. By treating these risks as additive, the current model may underestimate the compound impact where hazards reinforce each other (cascading effects). The analysis currently relies on secondary data sources, which may have limited spatial resolution for site-specific engineering. While robust for regional susceptibility mapping, the accuracy of the index is tied to the availability and precision of these national-level datasets.

Future research should move beyond linear summation toward dynamic systems analysis. This includes exploring compound risks, such as the "earthquake-landslide-tsunami" chain, to better understand how seismic activity multiplies the probability of coastal and slope failures in real-time. To improve the precision of the susceptibility maps, further studies should involve detailed field surveys and the integration of the latest high-resolution topographical and geotechnical data. Subsequent studies should explore the scientific meaning of

these risk patterns for infrastructure vulnerability theory. This includes analyzing how the absence of road redundancy in West Sulawesi impacts regional economic survivability during multi-hazard events

## 6. ACKNOWLEDGEMENT

The author expresses gratitude to Ministry of Higher Education, Science and Technology for their support in funding this research through a research grant PDP-Scheme (BIMA). Gratitude is also extended to the Research and Community Service Institute (LPPM) of Universitas Sulawesi Barat for facilitating the implementation of this research. The utmost appreciation is also extended to all parties who assisted, both in data collection, analysis, and scientific discussions, enabling the successful completion of this research.

## REFERENCES

- Ahmed, T., Rehman, K., Shafique, M., & Ali, W. (2023). GIS-based earthquake potential analysis in Northwest Himalayan, Pakistan. *Environmental Earth Sciences*, 82(4). <https://doi.org/10.1007/s12665-023-10798-2>
- Al Hakim, B., Prabawardani, D., Prijambodo, T., Setyaningrum, N., Bayu Sekaranom, A., & Aurora Shakyra, E. (2025). *Investigating Influencing Factors of Shoreline Changes in Bantul's Tourist Coastal Areas Using GIS and Satellite Data*. 21(1), 20–33. <https://doi.org/10.20884/1.oa.2025.21.1.1154>
- Alwi, M., Maharti, A. W. N., Rakhmadini, A., Prastiyawan, D., Rakhmatika, M., Adalya, N. M., Rosyida, Y. S., & Hizbaron, D. R. (2022). Pemetaan multi rawan bencana longsor, kekeringan, dan banjir di Kabupaten Semarang. *Majalah Geografi Indonesia*, 36 No.1, 19–31. <https://doi.org/10.22146/mgi.63231>
- Alwi, M., & Mutaqin, B. W. (2022). Geospatial mapping of tsunami susceptibility in Parangtritis coastal area of Yogyakarta, Indonesia. *Arabian Journal of Geosciences*, 15(15). <https://doi.org/10.1007/s12517-022-10608-2>
- Amri, M. R., Nurlambang, T., Supriyatna, & Anggrahita, H. (2020). Earthquake hazard model with AVS30 in Sukabumi, West Java Province. *IOP Conference Series: Earth and Environmental Science*, 561(1). <https://doi.org/10.1088/1755-1315/561/1/012049>
- Antara. (2021, March 1). 60 Titik Longsor Akibat Gempa Mamuju Telah Dibuka dan Bisa Diakses Masyarakat. <https://News.Okezone.Com/Read/2021/03/01/340/2369918/60-Titik-Longsor-Akibat-Gempa-Mamuju-Telah-Dibuka-Dan-Bisa-Diakses-Masyarakat>.
- Aslam, B., Ismail, S., & Maqsoom, A. (2020). *Geospatial mapping of Tsunami susceptibility of Karachi to Gwadar coastal area of Pakistan*. <https://doi.org/10.1007/s12517-020-05916-4>/Published
- Aslam, B., J. M., ZI, M., A, G., & IA, Q. (2017). GIS Mapping of Tsunami Susceptibility: Case Study of the Karachi City in Sindh, Pakistan. *Journal of Geography & Natural Disasters*, 07(01). <https://doi.org/10.4172/2167-0587.1000187>
- Biswas, S., & Sil, A. (2023). Tsunami Vulnerability Assessment and Multi-Criteria Decision Making Analysis of Eastern Coast of India Using GIS-Based Tools. *KSCE Journal of Civil Engineering*, 27(3), 1270–1287. <https://doi.org/10.1007/s12205-023-1493-y>
- BNPB. (2021). *Kajian Risiko Bencana Nasional Provinsi Sulawesi Barat 2022 - 2026*.
- BNPB. (2025). *Indeks Risiko Bencana Indonesia Tahun 2024* (Vol. 3). Badan Nasional Penanggulangan Bencana.
- Boerboom, L., Sharifi, A., Shamsudin, K., & Kabir, A. (2004, May 10). Spatial multi-criteria evaluation to enhance governance: changes in Malaysian planning. *Faculty of Geo-Information Science and Earth Observation*.
- BPS Kabupaten Majene. (2024). *Statistical Yearbook of Majene Regency 2024*.
- Castiglione, M., Capodici, M., Corsino, S. F., Cosenza, A., & Torregrossa, M. (2026). Multi-natural hazard mapping for critical infrastructures in complex territorial contexts: proposal of a novel methodological approach. *Journal of Environmental Management*, 400, 128767. <https://doi.org/10.1016/j.jenvman.2026.128767>

- Elmoulat, M., & Brahim, L. A. (2018). Landslides susceptibility mapping using GIS and weights of evidence model in Tetouan-ras-Mazari area (Northern Morocco). *Geomatics, Natural Hazards and Risk*, 9(1), 1306–1325. <https://doi.org/10.1080/19475705.2018.1505666>
- Foralisa Toyfur, M., Pribadi, K. S., Wibowo, S. S., & Sengara, W. (2017). *PEMILIHAN BENTUK MODEL PENILAIAN RISIKO BENCANA GEMPA BUMI UNTUK RUAS JALAN NASIONAL DI INDONESIA*. <http://www.emdat.be>,
- Hanafi, M. (2021, September 6). *Jalan Poros Majene-Mamuju tertutup longsor*. *Antaranews.Com*.
- Hanapi, M. (2020, January 12). *Trans Sulawesi di Majene Nyaris Putus Akibat Abrasi*. *Antaranews.Com*.
- Hanapi, M. (2023, June 21). *Jalan Trans Sulawesi Poros Mameju-Majene Tertutup Longsor*. *Antaranews.Com*.
- He, Y., & Beighley, R. E. (2008). GIS-based regional landslide susceptibility mapping: a case study in southern California. *Earth Surface Processes and Landforms*, 33(3), 380–393. <https://doi.org/10.1002/esp.1562>
- Himawan, & Utomo, A. (2022, October 11). *Longsor di Majene, Akses Jalan Trans Sulawesi Poros Mamuju Majene Terputus*. *Kompas.Com*.
- Hosseini, M., & Vayeghan, F. Y. (2008, October 12). A RISK MANAGEMENT MODEL FOR INTER-CITY ROAD SYSTEMS. *The 14th World Conference on Earthquake Engineering*.
- Jena, R., Pradhan, B., Almazroui, M., Assiri, M., & Park, H. J. (2023). Earthquake-induced liquefaction hazard mapping at national-scale in Australia using deep learning techniques. *Geoscience Frontiers*, 14(1). <https://doi.org/10.1016/j.gsf.2022.101460>
- Khan, H., Shafique, M., Khan, M. A., Bacha, M. A., Shah, S. U., & Calligaris, C. (2019). Landslide susceptibility assessment using Frequency Ratio, a case study of northern Pakistan. *Egyptian Journal of Remote Sensing and Space Science*, 22(1), 11–24. <https://doi.org/10.1016/j.ejrs.2018.03.004>
- Koks, E. E., Rozenberg, J., Zorn, C., Tariverdi, M., Vousdoukas, M., Fraser, S. A., Hall, J. W., & Hallegatte, S. (2019). A global multi-hazard risk analysis of road and railway infrastructure assets. *Nature Communications*, 10(1). <https://doi.org/10.1038/s41467-019-10442-3>
- Kristiawan, Y., Budianto, A., Suryadana, K. M., Muslim, D., & Zakaria, Z. (n.d.). *Landslide Susceptibility Mapping using Weight of Evidence In Mamuju Regency, West Sulawesi, Indonesia After West Sulawesi Earthquake on 14 th January 2021*. Retrieved <https://tanahair.indonesia.go.id/demnas/>
- Lee, S. (2019). Current and Future Status of GIS-based Landslide Susceptibility Mapping: A Literature Review. In *Korean Journal of Remote Sensing* (Vol. 35, Number 1, pp. 179–193). Korean Society of Remote Sensing. <https://doi.org/10.7780/kjrs.2019.35.1.12>
- Meilano, I., Salman, R., Susilo, S., Shiddiqi, H. A., Supendi, P., Lythgoe, K., Tay, C., Bradley, K., Rahmadani, S., Kristyawan, S., & Yun, S.-H. (2023). The 2021 MW 6.2 Mamuju, West Sulawesi, Indonesia earthquake: partial rupture of the Makassar Strait thrust. *Geophysical Journal International*, 233(3), 1694–1707. <https://doi.org/10.1093/gji/ggac512>
- Mustikaningrum, M., Widhatama, A. F., Widantara, K. W., Ibrohim, M., Hibatullah, M. F., Larasati, R. A. P., Utami, S., & Hadmoko, D. S. (2023). Multi-Hazard Analysis in Gunungkidul Regency Using Spatial Multi-Criteria Evaluation. *Forum Geografi*, 37(1), 35–45. <https://doi.org/10.23917/forgeo.v37i1.19041>
- Naufal, M., Nandini, M., Rahmanu, Y. A., Najib, D. W. A., Kusumaningrum, P. B., Ahyar, M. I., & Hizbaron, D. R. (2019). Disaster mapping as decision support system to decrease abrasion impact due to climate change in Bantul Coastal Area. *IOP Conference Series: Earth and Environmental Science*, 303(1). <https://doi.org/10.1088/1755-1315/303/1/012020>
- Pratama, D. N. D., Khakhim, N., Wicaksono, A., Musthofa, A., & Lazuardi, W. (2021). Spatio-temporal analysis of abrasion susceptibility effect on land cover in the coastal area of Bantul regency, Yogyakarta, Indonesia. *International Journal of Geoinformatics*, 17(4), 109–126. <https://doi.org/10.52939/ijg.v17i4.1961>
- PUSGEN. (2017). *Peta Sumber dan Bahaya Gempa Indonesia Tahun 2017*. Pusat Penelitian dan Pengembangan Perumahan dan Permukiman, Badan Penelitian dan Pengembangan, Kementerian Pekerjaan Umum.

- Rahayu, R. T. (2025). *Analisis dampak pembangunan infrastruktur JJLS terhadap peningkatan ekonomi Kabupaten Gunungkidul*.
- Römer, H., Willroth, P., Kaiser, G., Vafeidis, A. T., Ludwig, R., Sterr, H., & Revilla Diez, J. (2012). Potential of remote sensing techniques for tsunami hazard and vulnerability analysis—a case study from Phang-Nga province, Thailand. *Natural Hazards and Earth System Science*, 12(6), 2103–2126. <https://doi.org/10.5194/nhess-12-2103-2012>
- Safira, F. A., Muryani, C., & Tjahjono, G. A. (2022). Tsunami Susceptibility Analysis in Coastal Area Petanahan District, Kebumen Regency. *Jambura Geoscience Review*, 4(2), 110–122. <https://doi.org/10.34312/jgeosrev.v4i2.13938>
- Sambah, A. B., & Miura, F. (2018). *Geo Spatial Analysis for Tsunami Risk Mapping*. <https://doi.org/10.5772/intechopen.82665>
- Sambah, A. B., Miura, F., Guntur, & Fuad. (2018). Spatial multi criteria approach for tsunami risk assessment. *IOP Conference Series: Earth and Environmental Science*, 162(1). <https://doi.org/10.1088/1755-1315/162/1/012019>
- Sarkar, S., Kanungo, D. P., Patra, A. K., & Kumar, P. (2008). GIS based spatial data analysis for landslide susceptibility mapping. *Journal of Mountain Science*, 5(1), 52–62. <https://doi.org/10.1007/s11629-008-0052-9>
- Sholichin, M., Othman, F., Prayogo, T. B., & Rahardjo, S. S. P. (2024). Assessing Landslide susceptibility and formulating adaptation strategies in the Konto Watershed, East Java, Indonesia. *International Journal of Disaster Risk Reduction*, 113. <https://doi.org/10.1016/j.ijdr.2024.104797>
- Steinritz, V., Pena-Castellnou, S., Marliyani, G. I., & Reicherter, K. (2021). GIS-based study of tsunami risk in the Special Region of Yogyakarta (Central Java, Indonesia). *IOP Conference Series: Earth and Environmental Science*, 851(1). <https://doi.org/10.1088/1755-1315/851/1/012007>
- Tansel, B. (2025). Multi-hazard vulnerability and impact intensification: Interactive hazards and impact compounding in coastal areas. *International Journal of Disaster Risk Reduction*, 131, 105883. <https://doi.org/10.1016/j.ijdr.2025.105883>
- Triyatno, Anwar, S., Febriandi, & Rahmi, L. (2024). GIS BASED ON ANALYSIS OF EARTHQUAKE HAZARD LEVEL USING THE PGA IN SIBERUT–MENTAWAI ISLANDS REGENCY FOR SUSTAINABILITY IN DISASTER MITIGATION. *Journal of Sustainability Science and Management*, 19(12), 107–119. <https://doi.org/10.46754/jssm.2024.12.007>
- Ustaoğlu, B., İkiel, C., Atalay Dutucu, A., & Koç, D. E. (2021). Erosion Susceptibility Analysis in Datça and Bozburun Peninsulas, Turkey. *Iranian Journal of Science and Technology, Transaction A: Science*, 45(2), 557–570. <https://doi.org/10.1007/s40995-020-01053-5>
- Vakhshoori, V., & Zare, M. (2016). Landslide susceptibility mapping by comparing weight of evidence, fuzzy logic, and frequency ratio methods. *Geomatics, Natural Hazards and Risk*, 7(5), 1731–1752. <https://doi.org/10.1080/19475705.2016.1144655>
- Yi, Y., Zhang, Z., Zhang, W., Xu, Q., Deng, C., & Li, Q. (2019). GIS-based earthquake-triggered-landslide susceptibility mapping with an integrated weighted index model in Jiuzhaigou region of Sichuan Province, China. *Natural Hazards and Earth System Sciences*, 19(9), 1973–1988. <https://doi.org/10.5194/nhess-19-1973-2019>
- Zhou, S., Zhang, Y., Xing, J., Chen, C., & Fang, L. (2019). Earthquake-induced landslide susceptibility mapping: Application and Comparison of Frequency Ratio, Logistic Regression, Weight of Evidence and Support Vector Machine. *IOP Conference Series: Earth and Environmental Science*, 304(4). <https://doi.org/10.1088/1755-1315/304/4/042011>